where $c > 2$ is an arbitrary number and q is the number of first (also the last) vanishing coefficients of $T_{k-1}(z)$).

Step 3: Let $\nu_N = \text{var}\{T_N(1), T_{N-1}(1), \cdots, T_0(1)\}$ be the number of sign variations of $T_k(1)$ for $k = 0, 1, \cdots, N$. Then, $P(z)$ has $\alpha_N = N - \nu_N$ zeros inside unit circle. If $T_{m-1}(z) \equiv 0$ for some $m \geqslant 1$, then $P(z)$ has $\beta_N = 2\nu_N - m$ zeros on unit circle.
End.

For the application to 2-D stability testing, we have that $P(z) = z^M R(z)$ with $R(z)$ as in (3.1). Since $P(z)$ is symmetric, $T_{M-1}(z)$ (generated in step 2 of Algorithm 2) is identically zero. Hence, the number of zeros on unit circle for $R(z)$ is equal to $\beta_M = 2\nu_M - M$.

Algorithm 2 has a very nice feature since it uses almost the same number of additions and multiplications as Routh–Hurwitz table (which checks zero locations of a given polynomial with respect to imaginary axis) for same degree polynomial. It is very effective for zero testing of $R(z)$ (as in (3.1)) on unit circle. We present the following example to conclude this section.

Example 1: Consider $a(z_1, z_2)$ as given below:

$$a(z_1, z_2) = 4.4 + 2.598z_2 + 0.796z_1z_2 + 3.6z_1^2 + 0.199z_2^2 + 2.198z_1^2z_2 + 0.398z_1z_2^2 + 0.199z_1^2z_2^2.$$

By using 2-D stability testing algorithm, we have

$$a(0, z_2) = (2.2 + 0.199z_2)(2 + z_2) \neq 0, \qquad |z_2| \leqslant 1. \quad (3.6)$$

Using Cholesky factorization and DCT programs, we obtain

$$R(z) = 57.92 + 47.95(z + z^{-1}) + 31.17(z^2 + z^{-2}) + 13.69(z^3 + z^{-3}) + 2.534(z^4 + z^{-4}). \quad (3.7)$$

We thus set $P(z) = z^4 R(z)$ which is a polynomial of z with order $N = 8$. By using Algorithm 2, we obtain that $R(z)$ has four zeros on unit circle. This is justified by the fact

$$T_8(1) > 0, T_7(1) < 0, T_6(1) > 0, T_5(1) < 0, T_4(1) < 0, T_3(1) > 0, T_2(1) > 0, T_1(1) < 0, T_0(1) > 0. \quad (3.8)$$

Clearly, $\nu_N = 6$, and the number of zeros of $P(z)$ on unit circle is $\beta_N = 2\nu_N - N = 4$. Therefore, we conclude that the given 2-D system is unstable.

It is known that the root mapping method is quite popular for 2-D stability testing. The main idea is to calculate zeros of $a(z_1, e^{j\theta_k})$ for $\theta_k = 2k\pi/L$, with $k = 0, 1, \cdots, L-1$. Clearly, the accuracv of the stability testing directly relates to the length L e.g. Example 1, we need $L = 8192$ in order to conclude the instability of $a(z_1, z_2)$ which is very inefficient, recall that we have to compute L times of the zeros of $a(z_1, e^{j\theta_k})$.

References

[1] Y. Bistritz, "Zero location with respect to the unit circle of discrete-time linear system polynomials," *Proc. IEEE*, vol. pp. 1131–1142, Sept. 1984.

[2] W. H. Chen, C. H. Smith, and S. C. Fralick, "A fast computational algorithm for the discrete cosine transform," *IEEE Trans. Commun.* vol. COM-25, pp. 1004–1009, 1977.

[3] D. L. Davis, "A correct proof of Huang's theorem on stability," *IEEE Trans. Acoust., Speech, Signal Processing*, vol. ASSP-24, pp. 423–426, Oct. 1976.

[4] T. S. Huang, "Stability of two-dimensional recursive filters," *IEEE Trans. Audio Electroacoust.*, vol. AU-20, pp. 158–163, June 1972.

[5] E. I. Jury, "Stability of multidimensional scalar and matrix polynomial," *Proc. IEEE*, vol. 68, pp. 1018–1047, Sept. 1978.

[6] J. M. Orgtega, *Numerical Analysis — A Second Course*. New York: Academic, pp. 48.

[7] V. Ptak and N. J. Young, "A generalization of the zero location theorem of Schur and Cohn," *IEEE Trans. Automat. Contr.*, vol. AC-25, pp. 978–980, Oct. 1980.

Design of 2-D Digital Filters with Rectangular Passbands and Stopbands

ANDREAS ANTONIOU AND WU-SHENG LU

Abstract **—A modified version of a configuration proposed by Hirano and Aggarwal for the design of 2-D digital filters with rectangular stopbands is suggested and sufficient conditions for its correct operation are derived. On the basis of these conditions, it is shown that all possible stopbands can be achieved by using standard 1-D continuous low-pass, band-pass, or high-pass transfer functions.**

I. Introduction

Several types of two-dimensional (2-D) recursive digital filters can be designed, ranging from filters with circularly symmetric amplitude responses [1] to filters whose passband or stopbands are rectangular domains or combinations of rectangular domains [2], [3]. In the method of Hirano and Aggarwal [2], 2-D recursive filters whose passbands are rectangular are designed by cascading two 1-D low-pass, band-pass or high-pass filters or any other combination of two such filters. The design of 2-D recursive filters with rectangular stopbands, on the other hand, is achieved by using a configuration consisting of a cascade arrangement of 1-D filters of the type just described in parallel with a suitably designed all-pass filter.

In this paper, a modified version of stopband configuration of Hirano and Aggarwal is suggested and sufficient conditions for its correct operation are derived. On the basis of these conditions, it is shown that all possible stopbands can be achieved by using standard 1-D continuous low-pass, band-pass or high-pass transfer functions that can be obtained from the classical analog-filter approximations (Bessel, Butterworth, Chebyshev, and elliptic).

II. Configuration of Hirano and Aggarwal

The configuration of Hirano and Aggarwal for the design of 2-D recursive bandstop filters is illustrated in Fig. 1(a). Its transfer function is of the form

$$H(z_1, z_2) = H_{A1}(z_1) H_{A2}(z_2) - [H_1(z_1) H_2(z_2)]^2$$

where each of $H_1(z_1)$ and $H_2(z_2)$ can be a 1-D low-pass, band-pass, or high-pass transfer function and $H_{A1}(z_1)$ and $H_{A2}(z)$ are corresponding 1-D all-pass transfer functions whose poles are the same as those of $H_1(z_1)$ and $H_2(z_2)$, respectively.

If the all-pass transfer functions are of the form

$$H_{A1}(z_1) = \frac{z_1^n D_1(z_1^{-1})}{D_1(z_1)}$$

and

$$H_{A2}(z_2) = \frac{z_2^m D_2(z_2^{-1})}{D_2(z_2)}$$

where n and m are the orders of transfer functions $H_1(z_1)$ and $H_2(z_2)$, respectively, the configuration of Fig. 1(a) does not yield a bandstop filter in some of the nine possible cases identified in [2], as will now be demonstrated. Consider the low-pass and

Manuscript received March 21, 1988; revised April 19, 1989. This paper was recommended by Associate Editor Y. C. Jenq.

The authors are with the Department of Electrical and Computer Engineering, University of Victoria, Victoria, B.C., Canada V8W 2Y2.

IEEE Log Number 8931727.

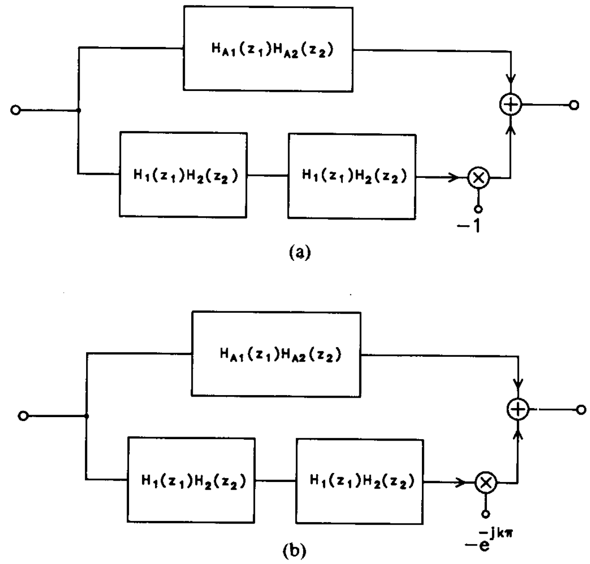

Fig. 1. (a) Configuration of Hirano and Aggarwal. (b) Modified configuration.

band-pass filters represented by the transfer functions

$$H_1(z_1) = \left.\frac{b_1}{s^2 + a_1 s + b_1}\right|_{s=(z_1-1)/(z_1+1)}$$

and

$$H_2(z_2) = \left.\frac{a_2 s}{s^2 + a_2 s + b_2}\right|_{s=(z_2-1)/(z_2+1)}$$

For these filters, the phase shift produced by the cascade arrangement of the low-pass and band-pass filters is not equal to the phase shift produced by the all-pass filters and, consequently, the gain of the cascade filters is not subtracted from that of the all-pass filters to produce a bandstop filter. This problem can be overcome by modifying the phase shift of the all-pass filter or, equivalently, by modifying the phase shift of the two cascaded filters.

III. Modified Configuration

Consider the modified configuration of Fig. 1(b) where k is an integer equal to -1, 0, or 1 depending on the types of transfer functions used for the 1-D filters. The transfer function of this configuration is

$$H(z_1, z_2) = H_{A1}(z_1) H_{A2}(z_2) - e^{-jk\pi}\left[H_1(z_1) H_2(z_2)\right]^2 \quad (1)$$

and as will be demonstrated below, it can realize all nine of the stopbands identified in [2].

If the transfer functions

$$H_1(z_1) = \frac{N_1(z_1)}{D_1(z_1)} = \frac{\sum_{i=0}^{n} a_{1i} z_1^i}{\sum_{i=0}^{n} b_{1i} z_1^i}$$

and

$$H_2(z_2) = \frac{N_2(z_2)}{D_2(z_2)} = \frac{\sum_{i=0}^{m} a_{2i} z_2^i}{\sum_{i=0}^{m} b_{2i} z_2^i}$$

represent two 1-D filters, then the 1-D all-pass transfer functions in (1) can be constructed as

$$H_{A1}(z_1) = \frac{z_1^n D_1(z_1^{-1})}{D_1(z_1)} = \frac{\sum_{i=0}^{n} b_{1(n-i)} z_1^i}{\sum_{i=0}^{n} b_{1i} z_1^i}$$

and

$$H_{A2}(z_2) = \frac{z_2^m D_2(z_2^{-1})}{D_2(z_2)} = \frac{\sum_{i=0}^{m} b_{2(m-i)} z_2^i}{\sum_{i=0}^{m} b_{2i} z_2^i}.$$

If we let

$$N_1(e^{j\omega_1 T_1}) = M_{N1}(\omega_1)\, e^{j\theta_{N1}(\omega_1)}$$
$$N_2(e^{j\omega_2 T_2}) = M_{N2}(\omega_2)\, e^{j\theta_{N2}(\omega_2)}$$
$$D_1(e^{j\omega_1 T_1}) = M_{D1}(\omega_1)\, e^{j\theta_{D1}(\omega_1)}$$

and

$$D_2(e^{j\omega_2 T_2}) = M_{D2}(\omega_2)\, e^{j\theta_{D2}(\omega_2)}$$

then (1) yields

$$H(e^{j\omega_1 T_1}, e^{j\omega_2 T_2}) = e^{j\psi_1(\omega_1,\omega_2)} - \frac{M_{N1}(\omega_1) M_{N2}(\omega_2)}{M_{D1}(\omega_1) M_{D2}(\omega_2)} e^{j\psi_2(\omega_1,\omega_2)} \quad (2)$$

where

$$\psi_1(\omega_1, \omega_2) = n\omega_1 T_1 + m\omega_2 T_2 - 2[\theta_{D1}(\omega_1) + \theta_{D2}(\omega_2)]$$

and

$$\psi_2(\omega_1, \omega_2) = -k\pi + 2[\theta_{N1}(\omega_1) + \theta_{N2}(\omega_2)] - 2[\theta_{D1}(\omega_1) + \theta_{D2}(\omega_2)].$$

Now if

$$\theta_{N1}(\omega_1) + \theta_{N2}(\omega_2) = \frac{1}{2}(k\pi + n\omega_1 T_1 + m\omega_2 T_2) \quad (3)$$

then

$$\psi_1(\omega_1, \omega_2) = \psi_2(\omega_1, \omega_2)$$

and so (2) assumes the form

$$H(e^{j\omega_1 T_1}, e^{j\omega_2 T_2}) = \left\{1 - \left[|H_1(e^{j\omega_1 T_1})|\,|H_2(e^{j\omega_2 T_2})|\right]^2\right\} e^{j\psi_1(\omega_1,\omega_2)}. \quad (4)$$

If

$$|H_1(e^{j\omega_1 T_1})| \approx \begin{cases} 0, & 0 \leqslant \omega_1 \leqslant \omega_{11} \\ 1, & \omega_{12} \leqslant \omega_1 \leqslant \omega_{13} \\ 0, & \omega_{14} \leqslant \omega_1 \leqslant \pi/T_1 \end{cases}$$

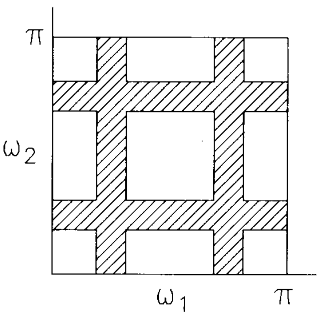

Fig. 2. Nine possible stopbands that can be obtained using the configuration in Fig. 1(b).

and

$$|H_2(e^{j\omega_2 T_2})| \approx \begin{cases} 0, & 0 \leqslant \omega_2 \leqslant \omega_{21} \\ 1, & \omega_{22} \leqslant \omega_2 \leqslant \omega_{23} \\ 0, & \omega_{24} \leqslant \omega_2 \leqslant \pi/T_2 \end{cases}$$

represent two 1-D bandpass filters, then

$$|H(e^{j\omega_1 T_1}, e^{j\omega_2 T_2})| \approx \begin{cases} 0, & \omega_{12} \leqslant \omega_1 \leqslant \omega_{13} \text{ and } \omega_{22} \leqslant \omega_2 \leqslant \omega_{23} \\ 1, & \text{otherwise} \end{cases}$$

and, therefore, the configuration of Fig. 1(b) realizes a 2-D filter whose amplitude response is complementary to that of the band-pass filter obtained by cascading the two 1-D band-pass filters. If each of the two cascade filters is allowed to be a low-pass, high-pass, or band-pass filter, the nine rectangular stopbands depicted in Fig. 2 can be obtained.

The configuration of Fig. 1(b) will complement the amplitude response of the two 1-D filters connected in cascade only if the phase angles of the numerator polynomials $N_1(z_1)$ and $N_2(z_2)$ are linear, according to (3). Following the approach of Antoniou [4, pp. 218–219], it can be shown that (3) will be satisfied under the following circumstances:

1) The coefficients of $N_1(z_1)$ and $N_2(z_2)$ have mirror image symmetry, that is, $a_{1i} = a_{1(n-i)}$ for $i = 0,1,2,\cdots,n$, and $k = 0$ in Fig. 1(b).
2) The coefficients of $N_1(z_1)$ and $N_2(z_2)$ have mirror image antisymmetry, that is, $a_{1i} = -a_{1(n-i)}$ for $i = 0,1,2,\cdots,n$, and $k = 0$ in Fig. 1(b).
3) The coefficients of $N_1(z_1)$ [or $N_2(z_2)$] have mirror image symmetry and those of $N_2(z_2)$ [or $N_1(z_1)$] have mirror image antisymmetry, and $k = -1$ or $+1$ in Fig. 1(b).

For 1-D discrete transfer functions obtained by applying the bilinear transformation to classical 1-D continuous transfer functions with zeros on the $j\omega$-axis or at the origin of the s plane (e.g., low-pass, high-pass, and band-pass transfer functions obtained from the Bessel, Butterworth, Chebyshev, or elliptic approximation) one of the above conditions is always satisfied, as can be easily demonstrated, and, consequently, any one of the nine stopbands in Fig. 2 can be readily achieved.

IV. Conclusions

A modified version of a configuration proposed by Hirano and Aggarwal for the design of 2-D digital filters with rectangular stopbands has been suggested and sufficient conditions for its correct operation have been derived. These conditions were then used to show that the nine possible stopbands can be realized by using standard 1-D continuous low-pass, band-pass, or high-pass transfer functions that can be derived from classical analog-filter approximations.

References

[1] J. M. Costa and A. N. Venetsanopoulos, "Design of circularly symmetric two-dimensional recursive filters," *IEEE Trans. Acoust., Speech, Signal Processing*, vol. ASSP-22, pp. 432–443, Dec. 1974.
[2] K. Hirano and J. K. Aggarwal, "Design of two-dimensional recursive digital filters," *IEEE Trans. Circuits Syst.*, vol. CAS-25, pp. 1066–1076, Dec. 1978.
[3] A. Antoniou, M. Ahmadi, and C. Charalambous, "Design of factorable lowpass 2-dimensional digital filters satisfying prescribed specifications," *Proc. Inst. Elec. Eng.*, vol. 128, pt. G, pp. 53–60, Apr. 1981.
[4] A. Antoniou, *Digital Filters: Analysis and Design*. New York: McGraw-Hill, 1979.

A Model-Based Approach for Filtering and Edge Detection in Noisy Images

A. RANGARAJAN, R. CHELLAPPA, AND Y. T. ZHOU

Abstract—We consider the problem of enhancement and edge detection on noisy, real-world images. The restoration and edge detection framework is based on an auto-regressive (AR) random field model. An edge is detected if the first and second directional derivatives and a local estimate of the variance at each point satisfy certain criteria. Due to the modeling assumptions, the directional derivatives are functions of the model parameters and of the neighboring pixels in a 3×3 window. When noise is present, a good estimate of the original from the noisy images improves the signal-to-noise-ratio and this results in better estimates of the directional derivatives. To avoid excessive computation, the problem of estimation of the original image and the model parameters is presented as a combination of a reduced update Kalman filter (RUKF) and an adaptive least squares parameter estimation algorithm. The restoration process is completed with a min–max replacement scheme to enhance edge strength. Since the edge detector operates on the processed image, restoration and edge detection cannot be performed simultaneously and the edge detector lags behind the restoration filter.

An orientation sensitive detector resulting from the use of an AR model may not detect edges of significantly different orientations. This is partially overcome by running four edge detectors on the four interior pixels of a 4×4 window; this corresponds to rotating the window in successive multiples of 90°. These intermediate results are stored at each point and the final result is the union of the outputs of the four edge detectors. Finally we present the results of applying this edge detector on noisy, real images. Comparisons with Haralick's facet model edge detector, Nevatia–Babu's line finder and Canny's edge detector are also given.

I. Introduction

Edge detection is an important topic to most researchers in the area of image understanding. A number of different techniques exist in the literature. A summary of many approaches to edge detection can be found in [1]. In this paper, we are interested primarily in edge detection on noisy images. When noise is

Manuscript received May 4, 1988; revised February 22, 1989. This paper was supported in part by the Joint Services Electronics Program under Contract F49620-85-C-0071. This paper was recommended by Associate Editor H. Gharavi.

The authors are with the Signal and Image Processing Institute, University of Southern California, Department of Electrical Engineering-Systems, Los Angeles, CA 90089.

IEEE Log Number 8931728.